



Optimization of Process Parameters by Taguchi Grey Relational Analysis in Joining Inconel-625 Through Microwave Hybrid Heating

Ravindra I. Badiger¹ · S. Narendranath¹ · M. S. Srinath²

Received: 4 August 2018 / Revised: 31 October 2018 / Accepted: 28 November 2018 / Published online: 10 December 2018
© Springer Science+Business Media, LLC, part of Springer Nature and ASM International 2018

Abstract

The quality of welded joints developed using microwave hybrid heating (MHH) technique is largely influenced by properties of the constituents employed in the process. This article investigates the influence of process parameters on tensile strength and flexural strength of Inconel-625 plates welded through MHH. Experiments were planned according to Taguchi L_{16} orthogonal array by considering three factors: separator, susceptor and filler powder particle size. Ultimate tensile strength and flexural strength of the specimens welded at 600 and 900 W were chosen as response characteristics. Application of Taguchi-based GRA has been effectively used to optimize multi-performance characteristics of the process. ANOVA results indicate that size of interface filler powder is the most significant factor in determining the joint strength followed by separator and susceptor. Further to corroborate the optimal parameter setting for maximum strength values, metallurgical characterization of the specimens is carried out through XRD and SEM. Specimens processed at 600 W exhibited superior properties compared to their counterparts developed at 900 W.

Keywords Microwave hybrid heating · Inconel-625 · Susceptor · Separator · EWAC · Grey relational analysis

Introduction

Nickel-based superalloy Inconel-625 is a solid solution invigorated by the additions of molybdenum and niobium in its nickel–chromium matrix. It is widely used in gas turbines, aircraft engines, marine industries and chemical power plants due to outstanding properties of strength, corrosion resistance and creep resistance at high temperatures. Conventionally welding of nickel-based super alloys has been successfully achieved by means of different fusion welding techniques including GTAW, EBW and laser beam welding [1, 2]. Most of these techniques are well matured in terms of technological developments and academic research. However, the large heat input through these conventional processes results in substantial change in base metal and fusion zone microstructure, which leads to diminish the mechanical properties [2, 3]. Further, the high operating

and maintenance costs associated with conventional welding processes also need to be considered. These processing limitations of conventional joining techniques therefore necessitate the development and introduction of novel techniques to weld advanced materials efficiently in a cost-effective manner and at the same time cater to the growing needs of the industry.

Microwave processing of materials is one of the pragmatic processes to produce parts with superior mechanical properties and improved microstructures. The process is also considered to be fast, clean and economical and consumes less power in comparison with existing techniques [4]. Walkiewicz et al. in 1988 demonstrated that metals in fine powdered form can be heated efficiently in a commercial microwave oven [5]. Processing of metals through microwave energy is difficult since microwaves get reflected when incident on metals, resulting in sparking which if neglected would damage the microwave source. However, bulk metals can be heated effectively using microwave hybrid heating (MHH) principles where the initial temperature of the metals is elevated by employing microwave-absorbing substance called susceptor. In recent days microwave processing of metallic-based materials has been carried out effectively by many researchers for the applications including cladding and

✉ Ravindra I. Badiger
rbadiger74@gmail.com

¹ Department of Mechanical Engineering, National Institute of Technology Karnataka, Surathkal, Karnataka, India

² Department of Industrial and Production Engineering, Malnad College of Engineering, Hassan, Karnataka, India

joining. Microwave processing of bulk metals was initiated in the year 2009 for joining of metals in a home microwave oven using hybrid heating technique [6]. This initial research paved the way for subsequent investigations on mechanical and metallurgical characterization of welded joints of various similar and dissimilar metals developed using MHH technique [7–11].

Various optimization techniques have been proposed to establish mathematical relationship between input parameters and performance characteristics in a welding process so as to produce the joint of desired quality. Taguchi-based grey relational analysis (GRA) is one of the popular techniques used by most of the researchers to optimize multiple responses in a process. Several researchers in recent past have used this technique to extend a skilful control over the uncertainty, partial information and multiple inputs. Lakshminarayanan and Balasubramanian [12] reported on Taguchi-based optimization of process parameters in friction stir welding of aluminium alloy. Tool rotational speed was more significant in deciding the tensile strength of the welded joints. Lin [13] optimized the process parameters in GTA welding of Inconel-718 to obtain the optimum depth to width ratio and penetration of weld bead using Taguchi, GRA and neural network techniques. Patel and Chaudhary [14] applied GRA to study the influence of process parameters on weld bead hardness during TIG and MIG welding of AISI 1020 steel. Ilo et al. [15] carried out the optimization of multiple quality characteristics in hard facing of mild steel substrate using Taguchi GRA. Ramesh and Suresha [16] used GRA to optimize the tribological parameters of carbon woven fabric reinforced epoxy hybrid composites with powdered Al_2O_3 and MoS_2 fillers. Taguchi-based GRA was applied to determine the optimum process parameters for multiple responses like wear rate, coefficient of friction and hardness. Prasad et al. [17] optimized the parameters of weld bead geometry of Inconel-625 welded joints produced using pulsed current plasma arc welding. Padmanabhan et al. [18] optimized the process parameters using GRA in TIG welding of alloy AZ31B with an objective of maximum tensile strength of the joint. In a subsequent study, Prasad et al. [19] reported on influence of input parameters on fusion zone grain size, hardness and UTS of Inconel-625 joints produced using pulsed current plasma arc welding. Objective was to minimize the grain size and maximize hardness and UTS. Srirangan and Paulraj [20] performed optimization of process parameters in GTAW of Incoloy-800 HT by GRA. Shanmugarajan et al. [21] carried out the optimization of laser welded P92 steel using Taguchi GRA technique to arrive at optimum set of parameters consisting of welding power, welding speed and focus plane position. Welding speed was the most significant parameter followed by laser power and focal length. Dwivedi and Sharma [22] studied the influence of process parameters on tensile strength of MS

joints developed using MHH. Process parameters considered were the input power, exposure time and temperature. In a recent research activity Hebbale and Srinath [23] developed cobalt-based clad on AISI-420 steel through MHH and optimized the process parameters influencing erosive wear using Taguchi method.

Reported works prove the efficacy of GRA technique for optimizing welding parameters; however, optimizing the predominant process parameters in welding of bulk metals using MHH has not been reported hitherto. In the present work, Taguchi-based GRA method has been proposed to optimize the process parameters (separator material, susceptor material and particle size of interface filler powder) influencing the mechanical properties of Inconel-625 welded joints produced using MHH. Experiments were carried out at two power levels (900 and 600 W). Tensile strength (UTS) and flexural strength (FS) of welded joints developed at these power levels were selected as output response characteristics. Further, XRD, microstructure and fractography studies of welded joints corresponding to optimal combination of process parameters have been carried out.

Experimentation

Welded joints in the present work were developed using a 900 W, 2.45 GHz domestic microwave oven (Make: LG Model: Solardom ML3483FRR) in atmospheric conditions without the aid of any shielding gas and clamping devices.

Material Details

Inconel-625 alloy plates of 6 mm thickness were joined through MHH using nickel-based powder EWAC as interface filler. Chemical composition and mechanical properties of as-received Inconel-625 alloy are presented in Table 1.

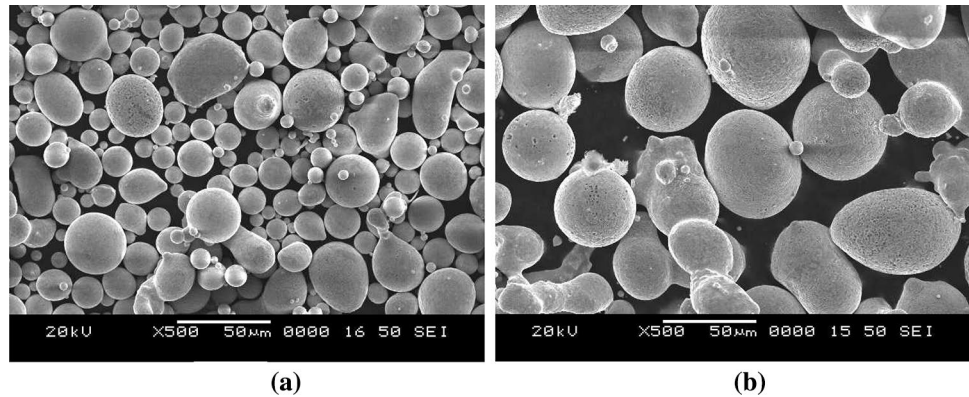
As-received EWAC powder was sieved to obtain two grades with average particle sizes (APS) 50 and 75 μm . SEM morphology of two grades of nickel-based powder is illustrated in Fig. 1a and b. Table 2 shows the chemical composition of EWAC powder. XRD analysis of EWAC powder was carried out to determine the elemental composition.

Multiple trials were carried out to determine the levels of the process parameters. The experiments were performed according to Taguchi L_{16} OA by considering three factors, separator with four levels and susceptor and interface filler powder size with two levels each. Multiple responses selected were UTS and FS of the joints developed at 900 and 600 W microwave power. Table 3 presents the process parameters and their levels.

Susceptors are materials that readily absorb the microwaves at room temperature; get heated by incident microwaves and transfer this heat to the target material through

Table 1 Composition and properties of base metal

Chemical composition, wt.%											
C	Si	Fe	Mo	W	Al	Co	Nb	Ti	V	Cr	Ni
0.058	0.283	4.451	8.195	0.1	0.005	0.1140	3.40	0.22	0.005	21.41	61.44
Mechanical properties											
Yield strength, MPa				Ultimate tensile strength, MPa				Hardness, HV			
699				945				260			

Fig. 1 SEM micrograph of EWAC powder with average particle size (a) 50 μm and (b) 75 μm **Table 2** Chemical composition of EWAC powder (wt.%)

Carbon	Silicon	Chromium	Nickel
0.2	2.8	0.17	Bal.

Table 3 Control factors and their levels

Code	Parameters	Levels			
		1	2	3	4
A	Separator	Gr	Gwl	GrF	GwlF
B	Susceptor	Coal	SiC
C	FP APS, μm	50	75

FP Filler powder, Gr Graphite, Gwl Glasswool, GrF Graphite with flux bed, GwlF Glasswool with flux bed. Flux used—UV420TT

conventional modes. Since SiC and coal are highly lossy and readily absorb microwaves at room temperature, both these materials were selected as susceptors.

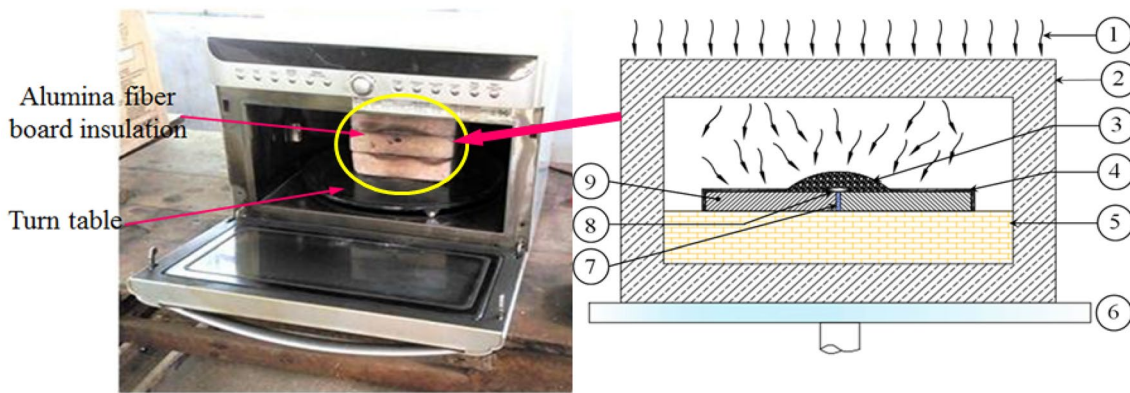
Separator is a thin sheet of refractory material used between susceptor and interface filler. Two types of separator materials graphite and glasswool were employed in the study. The objective behind selecting graphite and glasswool was to vary the microwave absorption characteristics at the joint interface as one of the materials is a very good microwave absorber (graphite) and the other is transparent to microwaves (glasswool). Interface filler paste was prepared

by blending nickel-based interface powder with epoxy resin and applied to the faying surfaces. Presence of chromium in Inconel-625 alloy promotes formation of oxide layer on the welded joint at elevated temperature. Wetting of interfacing surfaces to be joined is largely affected by the presence of this oxide layer. Therefore to reduce the effect of oxidation, flux UV420TT (Chemical composition: CaF_2 , $\text{CaO} + \text{MgO}$, $\text{Al}_2\text{O}_3 + \text{MnO}$ and $\text{SiO}_2 + \text{TiO}_2$) available in agglomerated form was used over the joint in combination with graphite and glasswool. The flux in granular form was further crushed and spread over the joint area prior to placement of separator.

Principle of Joining Bulk Metals Through MHH

Susceptor aided microwave joining of metallic materials is a distinctive application of suscepting material to selectively heat a localized area without affecting the remaining part of the metal.

Figure 2 shows the schematic of microwave welding setup in which alumina casket was used to minimize the heat loss. The surfaces of plates to be joined were cleaned with acetone and air-dried prior to joining. A suitable interface filler powder was mixed with an epoxy resin to form thick slurry and applied as sandwich layer between the surfaces to be joined. The advantage of using slurry is that it keeps the dry powder particles bound and prevents wastage of interface filler powder. However, the epoxy in the slurry



1. Microwave radiation; 2. Alumina foam insulation; 3. Susceptor; 4. Masking material; 5. Refractory base; 6. Turn table; 7. Filler powder; 8. Separator; 9. Base metal

Fig. 2 Schematic of experimental setup

gets evaporated at high temperature as the temperature of the interfacing layer increases due to microwave coupling. The bulk metallic pieces were covered with masking material so that they are not directly exposed to microwaves. As metals reflect microwaves at room temperature, they do not get heated on direct exposure to microwaves and result in sparking. To overcome this problem, a microwave-absorbing material called as susceptor is employed around the joint interface. As the exposure starts, susceptor couples with microwaves and gets heated to high temperature.

This heat from susceptor is transmitted to the interface filler powder by conventional mode of heat transfer via a separator plate, located between the base metal and susceptor. The separator prevents intermixing of susceptor and interface filler powder. When the interface temperature reaches a critical temperature T_C , interface powder particles couple with microwaves and start absorbing microwaves directly so as to cause self-heating. As the heating of the sample occurs in two modes; conventional mode (susceptor assisted) during initial phase and microwave heating in the second phase, the process is called mixed mode heating or **hybrid heating**. Thus, temperature at the joint interface rises to its melting point and a thin pool of melted metal forms between the interfacing surfaces and diffuses through a narrow dilution band in the joint zone. On cooling, a homogenous and solid joint is obtained through metallurgical bonding with the base metal.

Joint Characterization

Tensile test and 3-point bend test of the microwave welded Inconel-625 specimens were conducted with UTM (Make: Tinius Olsen, UK) to evaluate UTS and FS. The specimens were machined according to ASTM E8 and ASTM E190-92 guidelines, respectively, as shown in Fig. 3.

Tensile strength and flexural strength of the joints were evaluated with a uniform strain rate of 0.008 and 0.01 mm/s, respectively. Figures 4 and 5 illustrate, respectively, the photographs of tensile and 3-point bend test specimens produced (at 900 and 600 W) as per the L_{16} OA. XRD analysis of the welded joints was performed on BRUKER D8 Advance instrument with $\text{Cu-K}\alpha$ radiation. The scan rate was maintained at $1^\circ/\text{min}$ with scan range from 20° to 100° . Microstructures of the joints were investigated in SEM equipped with energy dispersive x-ray detector (JSM-6380 LA; JEOL, Japan).

Prior to microstructure study, the specimens were cut across the joint section using low-speed diamond wheel (Make: Chennai Metco). The candidate surfaces were polished with waterproof SiC abrasive papers using standard metallographic procedure followed by chemical etching with Marbles reagent.

Results and Discussion

Taguchi Method

Taguchi developed a technique based on orthogonal array (OA) of experiments which gives much reduced variance for the experiments with optimum settings of process parameters. OA is a statistical method of defining parameters that converts test areas into factors and levels. The Taguchi OA of experiments reduces the number experiments, time and money required for the experimentation. Generally, based on the factors and their levels large number of experiments have to be conducted as per conventional or full factorial design. Using Taguchi OA, the number of experiments can be reduced to 16 and it provides the information of experimental domain and their combinations. The purpose of

Fig. 3 Dimensions of (a) tensile test specimen (b) 3-point bend test specimen

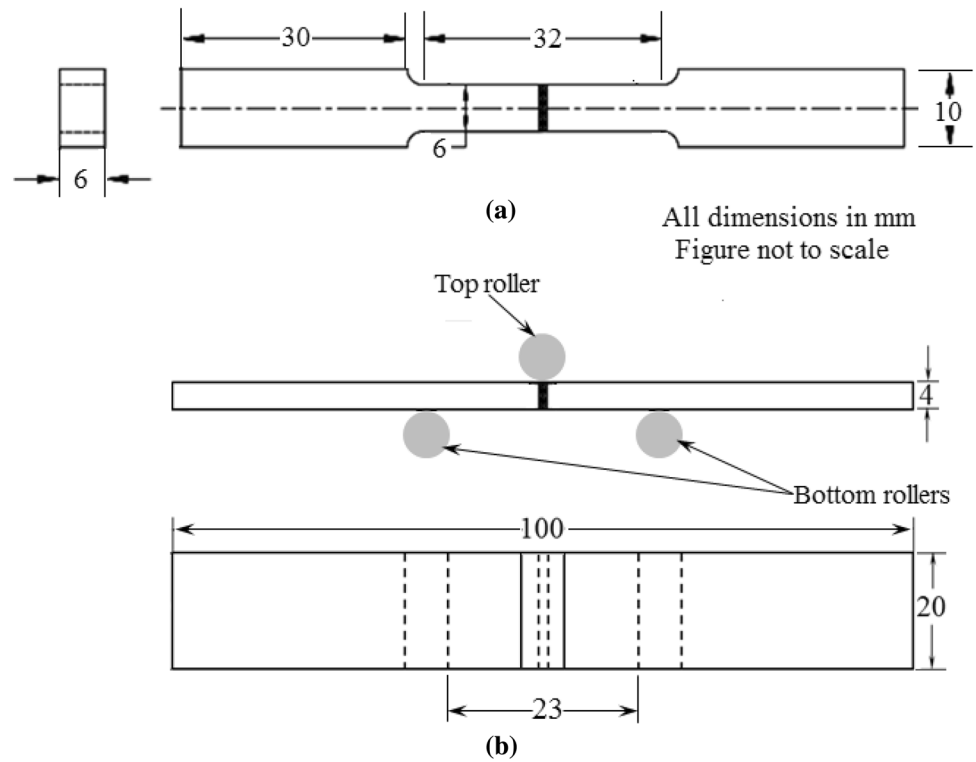
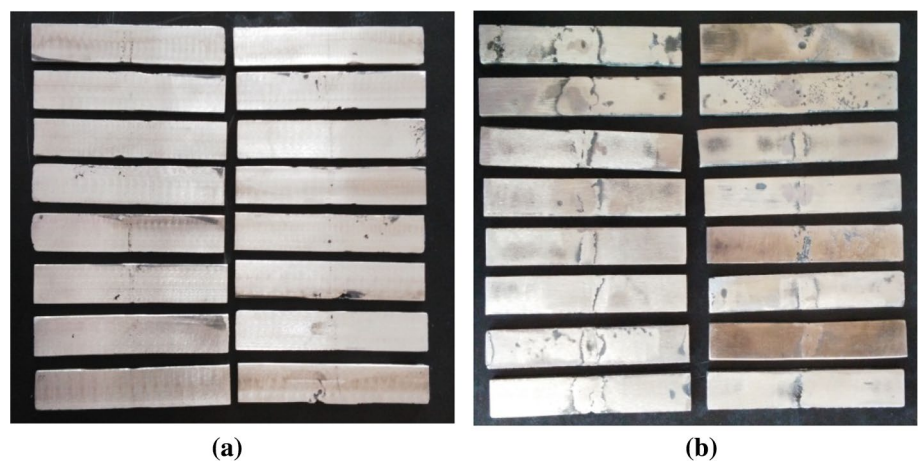


Fig. 4 ASTM E-8 standard tensile specimens produced at (a) 900 W (b) 600 W



Fig. 5 ASTM E-190-92 Standard 3-point bend test specimens (a) 900 W (b) 600 W



selecting an OA is to provide for optimum level of each factor using analysis of means and to determine the relative significance of individual factor using analysis of variance (ANOVA). Test design using OA creates an efficient and concise test suite with fewer test cases without compromising test coverage. An array name specifies the number of rows and columns and the levels of each column it has. The necessary number of experiments is selected based on the degrees of freedom (DF) of individual factors and the addition of DF of their interaction factors. The number of rows of an orthogonal array must be at least equivalent or greater than DF coupled with the selected factors, i.e. the control variables and their interactions. In general, total DF of each factor and the interactions of DF with an addition of errors DF are selected for total number of experiments to be conducted. In the present study 13 experiments have to be conducted as per total DF; however, the nearest array of design is L_{16} . Hence, L_{16} orthogonal array of experiments was selected for the experimentation.

Experiments were conducted by varying process parameters, which influence the process to obtain the required quality characteristics (Larger the better). Present study aims to maximize the ultimate tensile strength (UTS) and flexural strength (FS) of the welded joints developed through MHH. The results of experiments conducted as per Taguchi method using L_{16} OA are tabulated in Table 4.

Influence of Process Parameters on UTS and FS

The main effects plots for means of UTS and FS are shown in Fig. 6a–d. Observed strength values show a clear trend

that graphite separator has a positive effect to increase the UTS and FS. Graphite being a carbonaceous material possesses a high dielectric loss factor that readily absorbs microwave energy and provides efficient heating to the joint interface. Further it is noticed from Fig. 6b and d that a significant decrease in strength of the joint occurs between graphite and glasswool separators. Glasswool separator for both UTS and FS shows lowest response, while it is seen to be increased when glasswool is used in combination with flux for all the specimens regardless of power used for processing. As glasswool has extremely large penetration depth and transparent to microwaves (low loss Material) at room temperature, microwaves can easily pass through it and at the same time glasswool hinders the heat transfer from the susceptor to sample during the initial stage.

With increase in the temperature, glasswool melts (~ 750 °C) and a small volume of this melt may get included in the filler interface so as to form brittle phases resulting in lower joint strength. On the other hand, when flux is used along with glasswool, the fused flux bed acts as separator and forms a layer of slag on the molten filler interface which prevents oxidation resulting in improved joint strength. In a similar study Bansal et al. [10] joined Inconel-718 alloy through MHH wherein, UV420TT flux was used as a separator. However, no significant improvement in strength of specimens processed at 900 W was observed when flux used in combination with graphite.

It is evident from Fig. 6b and d that SiC exhibits better heating characteristics compared to coal when processing at 900 W. However, SiC requires a small warm-up time to couple with microwaves and thus initial high temperatures

Table 4 Experimental results using L_{16} OA

Expt. no.	Separator	Susceptor	FP APS, μm	Response at 600 W power		Response at 900 W power	
				UTS, MPa	FS, MPa	UTS, MPa	FS, MPa
1	A	B	C	347	615	309	562
2	1	1	2	318	516	247	434
3	1	2	1	312	573	345	537
4	1	2	2	236	429	257	476
5	2	1	1	326	651	234	429
6	2	1	2	290	560	228	310
7	2	2	1	304	456	295	526
8	2	2	2	281	393	182	418
9	3	1	1	376	612	304	519
10	3	1	2	298	418	254	464
11	3	2	1	345	559	315	551
12	3	2	2	318	461	280	483
13	4	1	1	353	665	320	427
14	4	1	2	309	485	228	355
15	4	2	1	296	530	290	540
16	4	2	2	249	402	279	414

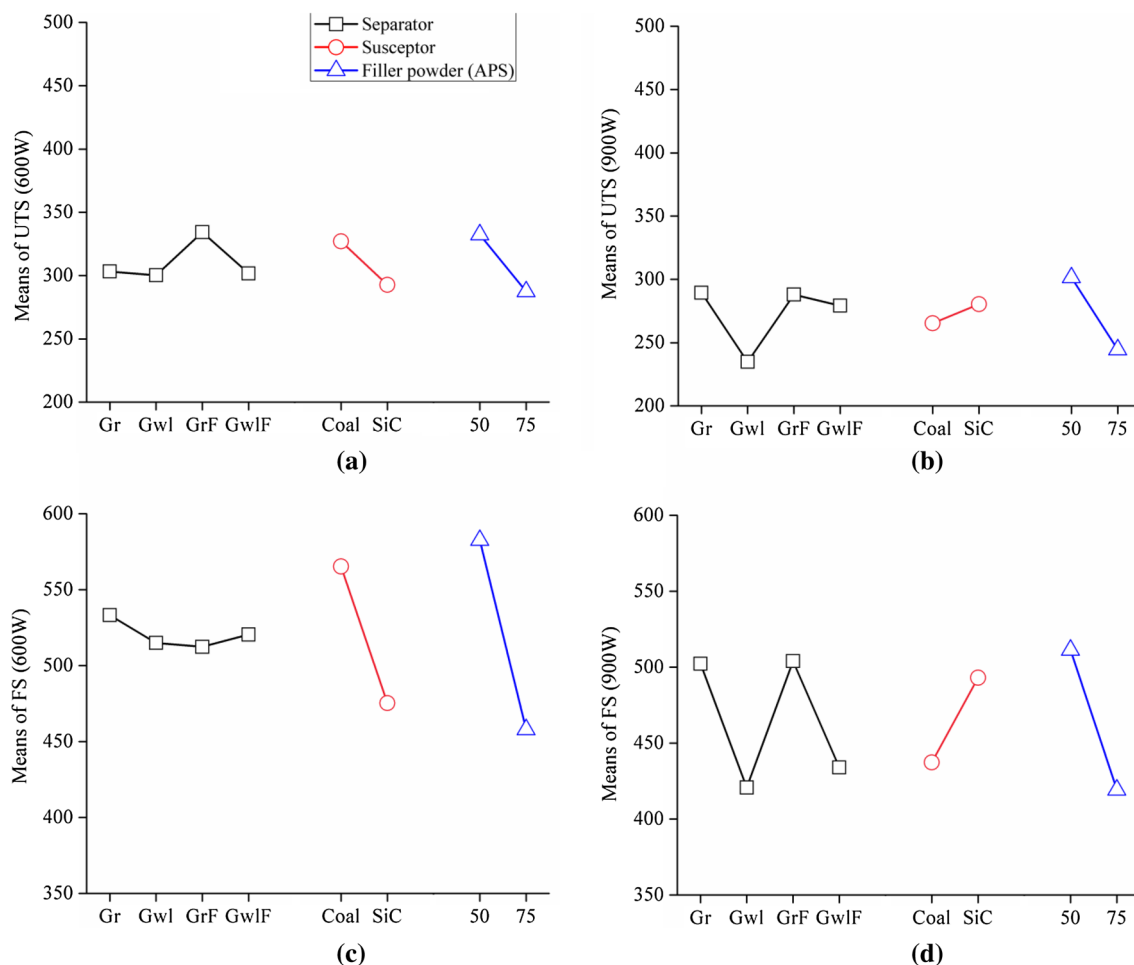


Fig. 6 Influence of process parameters on (a) UTS (600 W) (b) UTS (900 W) (c) FS (600 W) (d) FS (900 W)

are achieved at faster rate with coal as it is a carbonaceous material. With 900 W comparatively higher power, coal is burnt at faster rate and converted into ash. This may cause insufficient supply of heat at the joint zone resulting in lower strength of the joint. However, higher heating rates can be obtained with SiC due to its higher loss tangent value than coal. Further, it is seen that flexural strength of the specimens processed at 600 W power marginally improved with coal and graphite combination. It was also noticed from Fig. 6a–d that filler powder size of APS 50 micron exhibits better microwave heating characteristics for all the specimens irrespective of power input. This is due to the fact that microwave heating rate is largely affected by the electrical conductivity of the materials which in turn depends on the skin depth. Lower the skin depth, higher will be the conductivity and hence lower heating rate. As the interface powder particle size increases, the neighbouring particles come in contact with each other. As a result of this, electrical conductivity increases thereby decreasing the heating rate. Mondal et al. [24] and Yoshikawa et al. [25] demonstrated

that heating rate is largely affected by the particle size of the metallic powder and better heating rate is achieved with reduced particle size. At certain power level, as the particle size increases, heating rate decreases and with continued heating it becomes constant. Crane et al. [26] reported that it is not only the particle size but also the ratio of particle radius to the skin depth is more critical in deciding the heating rate. Bagha et al. [27] reported that with decreasing powder size there was significant increase in the tensile strength of SS-304 welded joints developed through MHH using EWAC powder. However, in addition, the combined effect of the type of susceptor and separator along with filler powder size has to be also considered.

Response Analysis

From Fig. 6a–d the optimal combination of process variables for obtaining best UTS values with the specimens processed at 600 and 900 W was observed as A3B1C1 (GrF, Coal and 50 micron) and A1B2C1 (Gr, SiC and 50 micron),

respectively. Similarly the optimal combination of process parameters for better FS of the Inconel-625 microwave-induced welded joints was determined as A1B1C1 (Gr, Coal and 50 micron) and A3B2C1 (GrF, SiC and 50 micron) when processed with 600 and 900 W, respectively. Further it was observed that filler powder APS was the most significant parameter followed by separator and susceptor. This is much obvious since in a typical microwave heating during the initial stage, filler powder requires susceptor assisted heating. Once the critical temperature is reached, thereafter heating primarily occurs due to microwave–metal powder surface interaction.

Analysis of Variance

To study the significance of process parameters towards each response characteristic, analysis of variance (ANOVA) was performed. ANOVA is a statistical tool used to ascertain the significance of process parameters on the performance measures at 95% confidence level. The general trend of contributing factors towards the process can be characterized by studying the main effects plot. ANOVA consists of sum of squares (SS), degrees of freedom (DF), mean square (MS), F-ratio and P value. The total SS represents the total variation in the response values and is the sum of the squared differences between the response value and the sample mean. The error SS is the sum of squared differences between the fitted values and the actual values and remains unexplained

by the fitted model. F-ratio is the statistical evaluation in which the test statistics has a F-distribution under the null hypothesis. F-statistics is ratio of mean square of parameter and the error. Highest F value signifies the highest percentage of contribution on the output responses. The *P* value for the test measures the probability of obtaining a F-ratio as large as what is observed, given that all parameters except the intercepts are zero.

Table 5 presents the ANOVA for UTS and FS which gives the information about major significant factor affecting output responses.

It was noticed that filler powder size is the most influencing factor affecting UTS and FS. This influence is identified from the F value and corresponding *P* values which is less than 0.05 (95% confidence). The interaction effect of all the process parameters does not have significant effect on the output responses; hence, it is pooled to error. The microwave power also significantly influences on the UTS and FS of welded joints since the welded samples at 600 W exhibit better characteristics due to the lower heat input associated with the process.

Multi-Objective Optimization Using GRA

In the second phase of this work, GRA was adopted to solve the problem of multiple quality characteristics since UTS and FS were not correlated mutually and each of the quality characteristics depended differently with control parameters.

Table 5 Results of ANOVA for UTS and Flexural strength

	Source	DF	Seq SS	Adj MS	F value	<i>P</i> value	Remarks
UTS (specimens processed at 600 W)	Separator	3	3186.8	1062.3	2.69	0.103	Insignificant
	Susceptor	1	4761	4761	12.04	0.006	Significant
	Filler powder	1	8100	8100	20.49	0.001	Significant
	Error	10	3954	395.4
	Total	15	20,001.8
UTS (specimens processed at 900 W)	Separator	3	8027.7	2675.9	4.91	0.024	Significant
	Susceptor	1	885.1	885.1	1.62	0.231	Insignificant
	Filler powder	1	13,053.1	13,053.1	23.95	0.001	Significant
	Error	10	5451.1	545.1
	Total	15	27,416.9
FS (specimens processed at 600 W)	Separator	3	1027	342	0.14	0.931	Insignificant
	Susceptor	1	32,310	32310	13.58	0.004	Significant
	Filler powder	1	62,126	62,126	26.11	0.000	Significant
	Error	10	23,797	2380
	Total	15	119,259
FS (specimens processed at 900 W)	Separator	3	23,387	7796	8.10	0.005	Significant
	Susceptor	1	12,377	12,377	12.87	0.005	Significant
	Filler powder	1	33,948	33,948	35.29	0.000	Significant
	Error	10	9620	962
	Total	15	79,331

Therefore, Taguchi method of optimization was extended for the complete evaluation of multiple quality characteristics in joining of Inconel-625 alloy using MHH technique through GRA.

In the first step of GRA pre-processing of data is performed so as to normalize the raw data. Normalization of S/N ratio (larger is better) for multiple quality characteristics was computed using Eq 1 and is tabulated in Table 6.

In the Taguchi OA design, there are controllable and non-controllable factors influencing the product output characteristics. The S/N ratio (signal–noise ratio) considers both mean and variability of the experimental results into account. It depends on the quality characteristic of output responses/ results and environmental factors. Once the S/N ratio is calculated for all the experimental trials, it converts the entire parameters unit into single standard decibel unit (DB) so that the analysis of data becomes simpler.

$$Z_{ij} = \frac{y_{ij} - \min(y_{ij}, i = 1, 2 \dots n)}{\max(y_{ij}, i = 1, 2 \dots n) - \min(y_{ij}, i = 1, 2 \dots n)} \quad (1)$$

where y_{ij} is S/N ratio for the i th performance characteristic considered in j th experiment, Z_{ij} is the normalized S/N ratio of i th performance characteristic in j th experiment.

Grey relational coefficient is calculated using Eq 2 to express the relationship between ideal and actual normalized results [28]. Prior to this, the deviation sequence for reference sequence and comparability sequence are computed.

$$\xi_i(k) = \frac{\Delta_{\min} + \zeta \Delta_{\max}}{\Delta_{oi}(k) + \zeta \Delta_{\max}} \quad (2)$$

where $\Delta_{oi}(k)$ is the deviation sequence of reference and comparability sequence expressed by Eq 3.

$$\Delta_{oi}(k) = \|y_0(k) - y_i(k)\| \quad (3)$$

$$\Delta_{\min} = \min_j \in i \quad \min_k \|y_0(k) - y_j(k)\| \quad (4)$$

$$\Delta_{\max} = \max_j \in i \quad \max_k \|y_0(k) - y_j(k)\| \quad (5)$$

$y_0(k)$ is the sequence and $y_j(k)$ the comparability sequence. ζ is distinguishing coefficient. Smaller the value of ζ , larger is the distinguishing ability. Value of ζ is assumed in the range $0 < \zeta < 1$. In the present study $\zeta = 0.5$ is used.

Grey relational grade is computed by taking the average of grey relational coefficients corresponding to each performance characteristic. The overall performance characteristic of multiple response process depends on the grey relational grade computed using Eq 6 [28]. Grey relational coefficient and corresponding grades for each experiment of L_{16} OA are summarized in Table 7.

$$\gamma_i = \frac{1}{n} \sum_{k=1}^n \xi_i(k) \quad (6)$$

where γ_i is the grey relational grade corresponding to j th experiment and k denotes the number of performance characteristics.

Effect of each process parameter can be separated out at different levels on grey relational grade as the design of experiments is orthogonal. Means of grey relational grade for each

Table 6 Pre-processing of data by normalizing S/N ratio

Expt. no.	S/N ratio (raw data)				S/N ratio normalized			
	UTS (600 W)	UTS (900 W)	FS (600 W)	FS (900 W)	UTS (600 W)	UTS (900 W)	FS (600 W)	FS (900 W)
1	50.81	49.80	55.78	54.99	0.83	0.83	0.85	1.00
2	50.05	47.85	54.25	52.75	0.64	0.48	0.52	0.57
3	49.88	50.76	55.16	54.60	0.60	1.00	0.72	0.92
4	47.46	48.20	52.65	53.55	0.00	0.54	0.17	0.72
5	50.26	47.38	56.27	52.65	0.69	0.39	0.96	0.55
6	49.25	47.16	54.96	49.83	0.44	0.35	0.67	0.00
7	49.66	49.40	53.18	54.42	0.54	0.76	0.28	0.89
8	48.97	45.20	51.89	52.42	0.37	0.00	0.00	0.50
9	51.50	49.66	55.74	54.30	1.00	0.80	0.84	0.87
10	49.48	48.10	52.42	53.33	0.50	0.52	0.12	0.68
11	50.76	49.97	54.95	54.82	0.82	0.86	0.67	0.97
12	50.05	48.94	53.27	53.68	0.64	0.67	0.30	0.75
13	50.96	50.10	56.46	52.61	0.86	0.88	1.00	0.54
14	49.80	47.16	53.71	51.00	0.58	0.35	0.40	0.23
15	49.43	49.25	54.49	54.65	0.49	0.73	0.57	0.93
16	47.92	48.91	52.08	52.34	0.12	0.67	0.04	0.49

level of factors considered are highlighted in Table 8. The optimum combination observed from Table 9 was A3B1C1, i.e. GrF separator followed by coal susceptor and 50 micron (APS) filler powder. Influence of control factors is shown in Fig. 7 through main effects plot of grey relational grade. Use of coal as susceptor and finer filler powder size contribute in increasing the grey relational grade. Experiment number 9 was found to present the optimum performance characteristics among sixteen experiments since it has highest grey relational grade.

ANOVA of grey relational grade is presented in Table 9. The study shows that filler powder (APS) and separator are the significant parameters that determine 77% and 13% variability, respectively.

Confirmation Test

The confirmation test for the obtained optimum process parameters with its levels was performed once again to confirm the quality characteristics of microwave welded Inconel-625 alloy joints. Table 7 presents the highest grey relational grade highlighting the combination of initial process parameters as A3B1C1 (Experiment No. 9) which gives the best multiple performances among sixteen experiments. Table 10 shows comparison between experimental results for optimal condition (A3B1C1) and that of predicted results for optimal condition (A3B1C1). Confirmation experiment results indicate a good agreement between the experimental and predicted results. The predicted values were estimated by Eq 7.

Table 7 Calculated grey relational coefficient, grey relational grade and rank

Expt. no.	Grey relational coefficient				Grey relational grade	Rank
	UTS (600 W)	UTS (900 W)	FS (600 W)	FS (900 W)		
1	0.74	0.74	0.77	1.00	0.81	2
2	0.58	0.49	0.51	0.54	0.53	11
3	0.56	1.00	0.64	0.87	0.77	5
4	0.33	0.52	0.37	0.64	0.47	12
5	0.62	0.45	0.93	0.52	0.63	7
6	0.47	0.44	0.60	0.33	0.46	13
7	0.52	0.67	0.41	0.82	0.61	8
8	0.44	0.33	0.33	0.50	0.40	16
9	1.00	0.72	0.76	0.79	0.82	1
10	0.50	0.51	0.36	0.61	0.50	10
11	0.73	0.78	0.60	0.94	0.76	4
12	0.58	0.61	0.42	0.66	0.57	9
13	0.79	0.81	1.00	0.52	0.78	3
14	0.54	0.44	0.45	0.39	0.46	14
15	0.49	0.65	0.54	0.88	0.64	6
16	0.36	0.60	0.34	0.49	0.45	15

Table 8 Response table for grey relational grade

Parameter	Level				Total Mean of GRG	Rank
	1	2	3	4		
A	0.644	0.525	0.66	0.58	0.603	2
B	0.623	0.583	3
C	0.727	0.479	1

Table 9 ANOVA of grey relational grade

Source	DF	Seq SS	Adj MS	Test F	P value	Remarks
Separator	3	0.046	0.015	8.36	0.004	Significant
Susceptor	1	0.006	0.006	3.53	0.090	Insignificant
Filler powder	1	0.246	0.246	134.26	0.000	Significant
Error	10	0.018	0.0018
Total	15	0.317

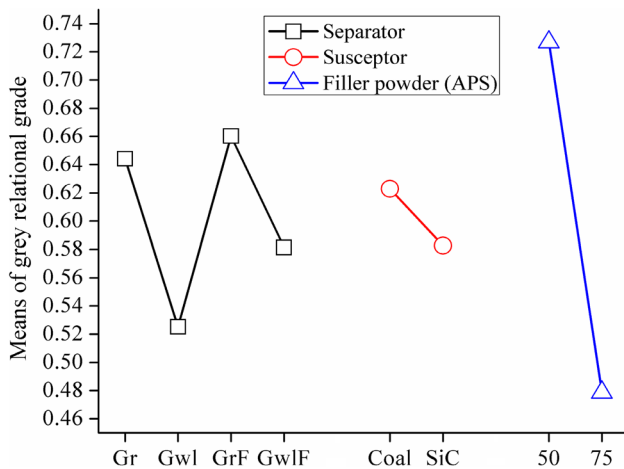


Fig. 7 Influence of control factors

Table 10 Predicted and confirmation test results for optimal condition A3B1C1

Response characteristics	Predicted, MPa	Experimental, MPa
UTS (600 W)	374	382
UTS (900 W)	309	322
FS (600 W)	620	623
FS (900 W)	523	517

$$\text{Predicted response} = \text{Avg.}(A3) + \text{Avg.}(B1) + \text{Avg.}(C1) - 2(\text{Mean response } Y_{ij}) \quad (7)$$

where Y_{ij} is the value of response.

Metallurgical Observations

After the confirmation experiment, the welded specimens were subjected to metallurgical characterization through XRD and SEM.

XRD Observations

XRD patterns obtained for the specimens produced at 600 and 900 W are shown in Fig. 8a and b, respectively. Dominant peaks of nickel along with the formation of various carbides and intermetallic compounds can be clearly seen. The presence of chromium carbide (CrC), niobium carbide (NbC), molybdenum carbide (Mo_2C), and intermetallic compounds nickel niobium (NiNb), along with NiO was noticed. Since chromium has a good affinity with carbon at elevated temperatures, these elements react to form

respective carbides. The equilibrium partition coefficient of niobium in nickel-based alloys is below one; thus it easily precipitates into interdendritic region during solidification to produce niobium carbide [29]. Formation of intermetallic elements is due to the fact that various alloying elements that were independent in the interface powder during heating react with each other resulting in combined intermetallic phases. As dielectric properties are dependent on solid-state transformations, the presence of these carbides and intermetallics promotes better coupling of interface powder with microwaves.

Approximate amounts of various phases existing in the weld zone were further determined by using intensity peaks of the respective phases. Tables 11 and 12 present the peak intensity values of phases existing in the joint zone. Pelemedu et al. [30] proposed a method to determine the approximate amount of phase present in any material through normalized intensity ratio (NIR). Accordingly, Eq 8 was used to determine the NIR of phase 1 (Ni) in the joint zones of specimens developed using 600 and 900 W, respectively. Similarly, the NIR of the other phases can be ascertained using these equations.

$$\text{NIR}_1 = \frac{I_1 - I_{\text{back}}}{I_1 + I_2 + I_3 + I_4 + I_5 + I_6 + I_7 + I_8 - 8(I_{\text{back}})} \quad (8)$$

where $I_1, I_2, I_3, I_4, I_5, I_6, I_7$ and I_8 are the corresponding phase intensities of phases 1–8 as seen from Fig. 8a and b. I_{back} is the background intensity. In case of multiple peaks of the same element/phase, highest peak conforming to that particular phase is used for determination of NIR. The NIR values indicated may not give precise amount of phases, though a relative approximation of amount of phases could be certainly predicted. It is seen from Tables 11 and 12 that during joining of Inconel-625 through MHH at 600 and 900 W, approximately 45.66 and 55.33%, respectively, of the starting EWAC powder was converted into various carbides and intermetallic phases.

SEM Observations

Figure 9a and b shows the SEM micrographs of Inconel-625 alloy welded using MHH at 600 and 900 W, respectively. Complete metallurgical bonding of powder particles can be observed clearly which resulted in a cellular structure in both the cases. However, lower segregation in the interdendritic region is observed with specimen processed at 600 W.

In order to determine the elemental composition, EDS analysis was carried out at interior of the grain and at grain boundaries as illustrated in Figs. 10 and 11. Elemental composition at point 1 in Fig. 10 indicates relatively tough phase compared to the elemental composition at point 2 where secondary precipitation is observed. Figure 11

Fig. 8 XRD patterns of the Inconel-625 welded joints developed at (a) 600 W and (b) 900 W

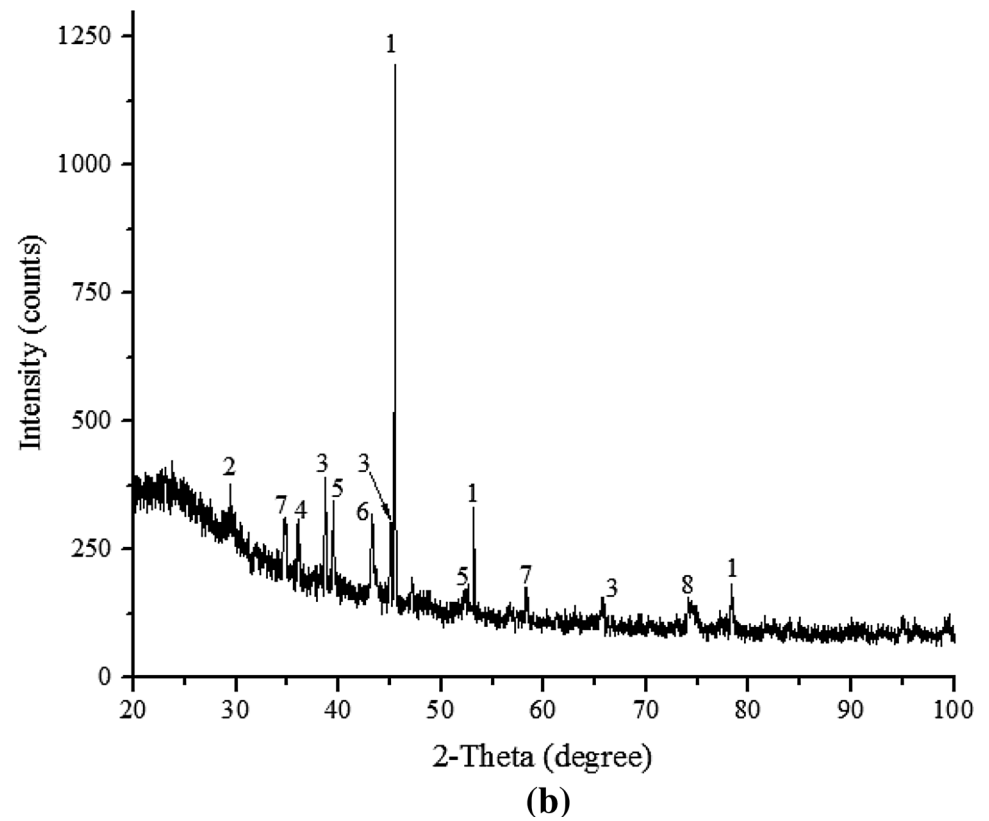
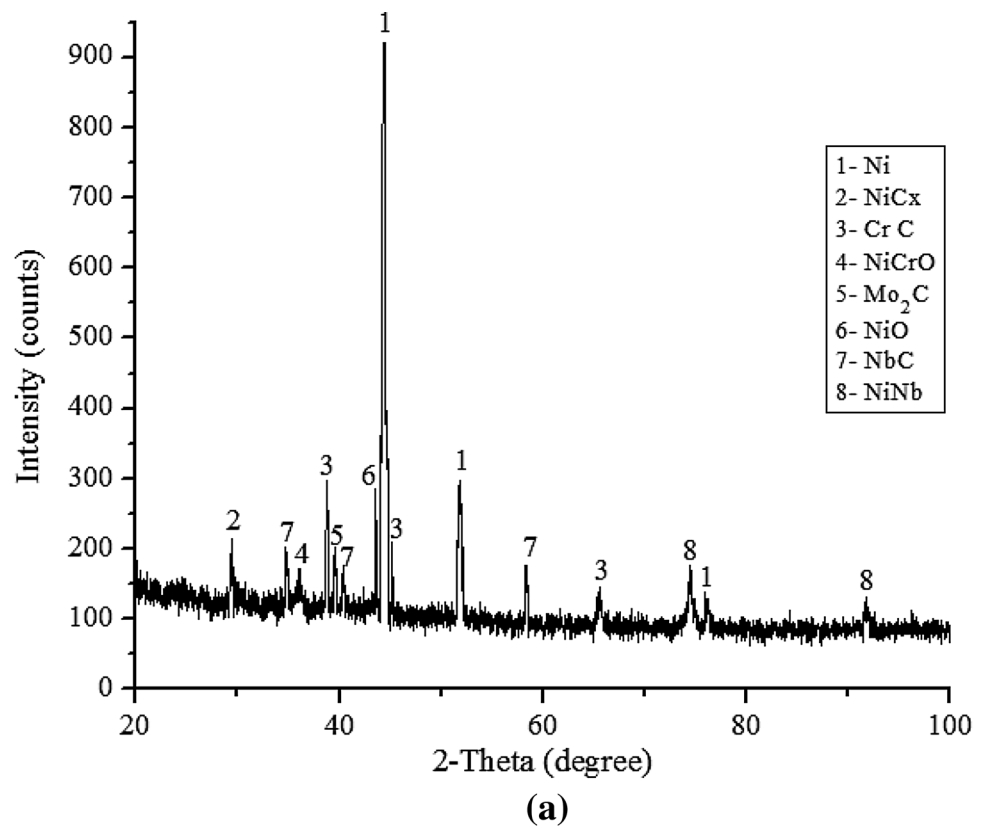
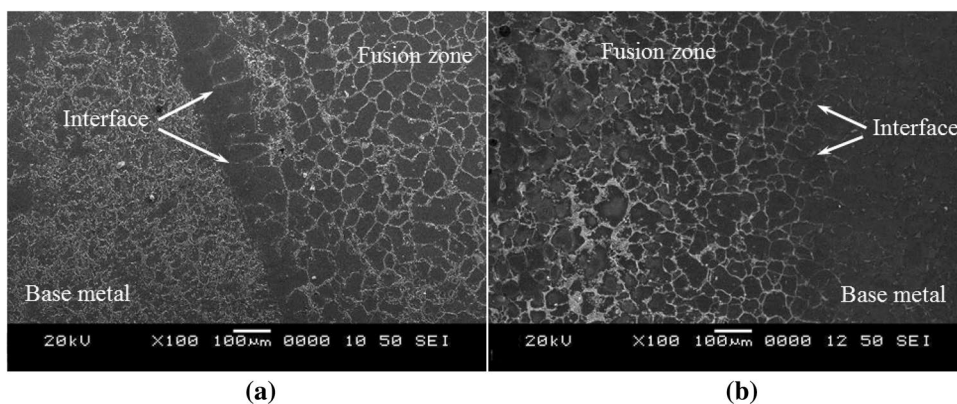


Table 11 Relative phase intensities in the joint zone of the specimen processed at 600 W

Sl. no.	Phase	I_1	I_2	I_3	I_4	I_5	I_6	I_7	I_8	I_{back}	NIR%
1	Ni	923	125	54
2	NiCx	...	213	125	5.96
3	CrC	298	125	11.7
4	NiCrO	172	125	3.1
5	Mo ₂ C	203	125	5.2
6	NiO	287	125	10.9
7	NbC	202	...	125	5.2
8	NiNb	178	125	3.6

Table 12 Relative phase intensities in the joint zone of the specimen processed at 900 W

Sl. no.	Phase	I_1	I_2	I_3	I_4	I_5	I_6	I_7	I_8	I_{back}	NIR%
1	Ni	1198	125	44.5
2	NiCx	...	377	125	10.45
3	CrC	390	125	11.0
4	NiCrO	310	125	7.6
5	Mo ₂ C	347	125	9.2
6	NiO	318	125	8.0
7	NbC	315	...	125	7.8
8	NiNb	156	125	1.28

Fig. 9 SEM micrograph of Inconel-625 welded joints obtained after confirmation experiment processed at (a) 600 W (b) 900 W power levels

shows the EDS analysis for the specimen welded at 600 W wherein clear grain boundaries in the fusion zone can be identified which is attributed to uniform heating associated with the process. Elemental composition at the interior of the grain (point 3) in Fig. 11 is almost the same as that observed at point 1 in Fig. 10.

However, at grain boundaries comparatively less amount of segregation is observed (point 4) in Fig. 11 than that observed at point 2 in Fig. 10. EDS analysis at the grain boundaries in Figs. 10 and 11 revealed higher Si and Fe contents that promote formation of Laves Phase.

The presence of Laves phase is unfavourable to the strength of welded joint, since it consumes the considerable amount of useful alloying elements required for strengthening of the matrix phase. At elevated temperature, the diffusion of niobium and molybdenum takes place from the base metal to the fusion zone that promotes the formation of Laves phase. Laves phase requires at least 10–12% Nb to form, and the volume of Laves phase, its composition and distribution in the weld microstructure are strongly influenced by the solidification condition [31]. In the present study, as revealed by EDS analysis the

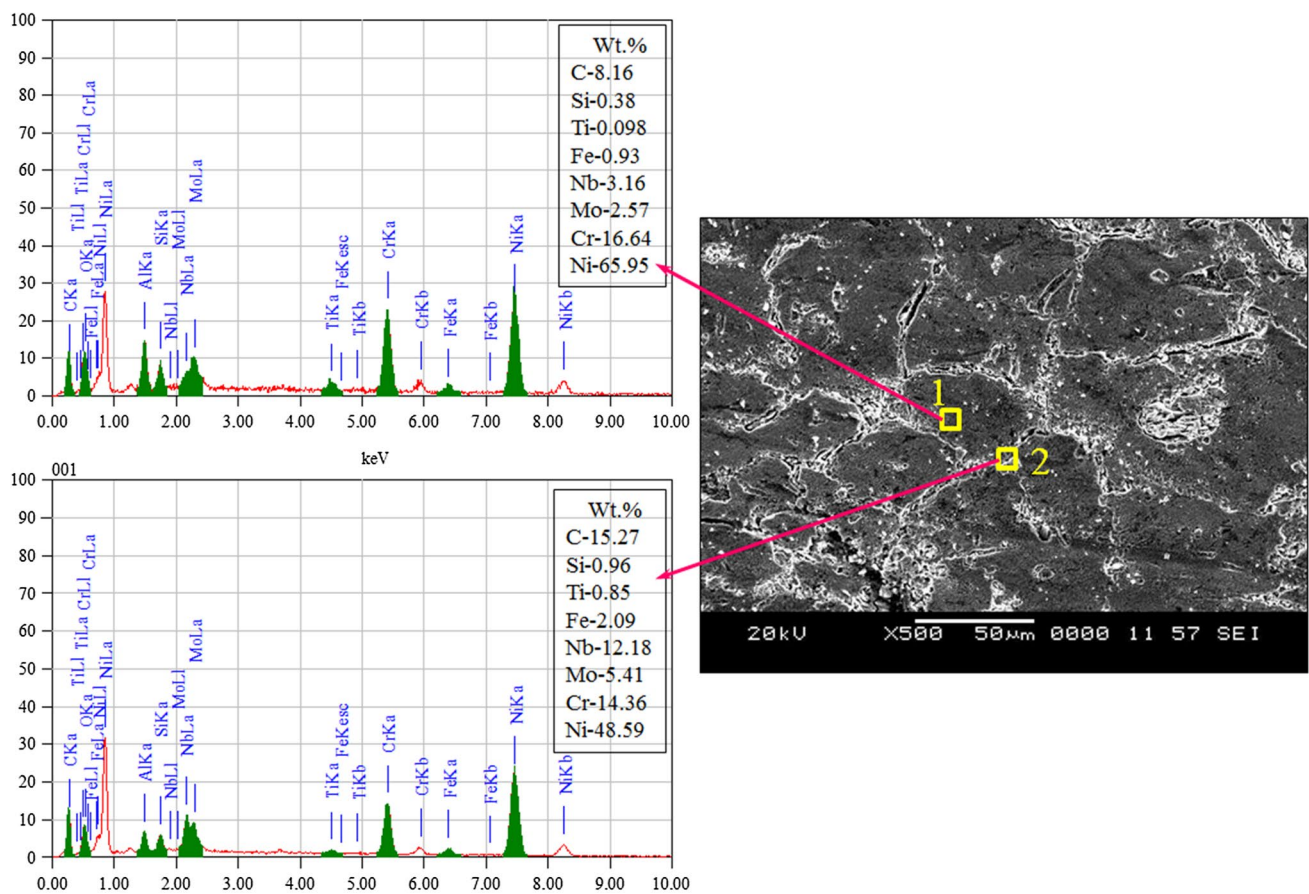


Fig. 10 SEM micrograph and EDS analysis in fusion zone of Inconel-625 specimen welded at 900 W

composition of Si is also reasonably high which further encourages the formation of Laves phase in interdendritic regions.

During processing materials through MHH, volumetric heating of the joint interface takes place followed by slow cooling. Microwave heating occurs due to frictional heat generated through dipolar rotation and with the seizure of microwave power the dipoles come to rest instantaneously. However, due to a slightly lower cooling rate associated with specimens processed at 900 W, higher amount of segregation is observed in the fusion zone and its vicinity.

The amount of Laves phase formed in the joints processed at 600 and 900 W was determined through image analysis as highlighted in Table 13. It was noticed that the amount of Laves phase and its niobium content were substantially lower in welded joints developed at 600 W compared to those produced at 900 W power levels. This is attributed to lower heat input associated with 600 W power followed by

rapid cooling which results in lower amount of Nb segregation and less time available for redistribution of solute.

In order to assess the mode of failure, fractured specimens were subjected to fractography analysis using SEM. Figure 12a and b presents the SEM micrographs of fractured surfaces of specimens that were processed at 600 and 900 W. In both the cases mixed mode type of fracture was observed. Specimen processed at 600 W exhibited the formation of dimples in the fusion zone (Fig. 12a) which shows that the specimen experiences a large amount of plastic deformation before failure. On the other hand, in Fig. 12b development of cracks is observed which is attributed to the presence of brittle phases at grain boundaries that act as source for crack initiation as the specimen deforms. Thus, specimens processed at 600 W exhibited superior mechanical properties as well as metallurgical characteristics compared to those processed at 900 W.

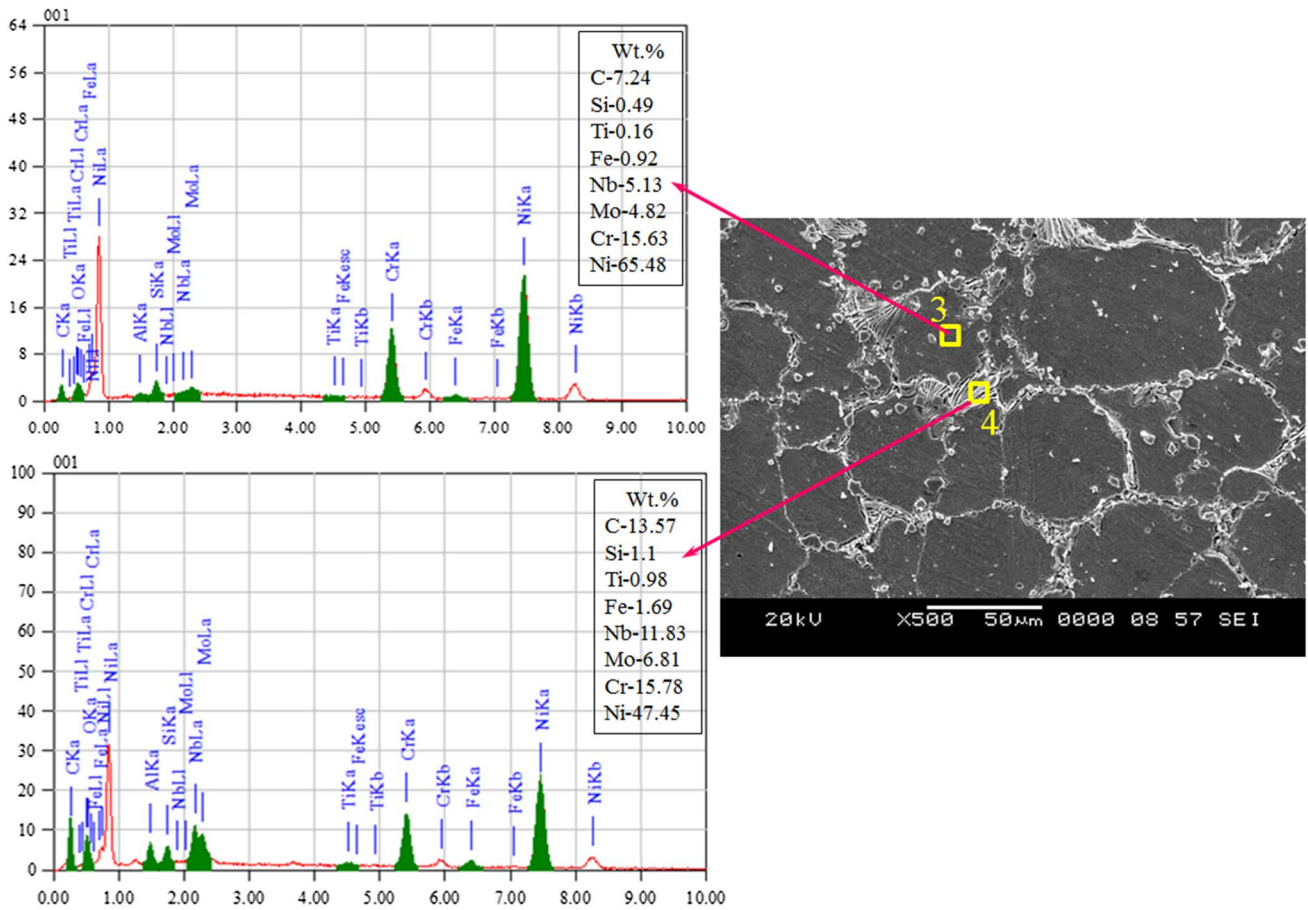
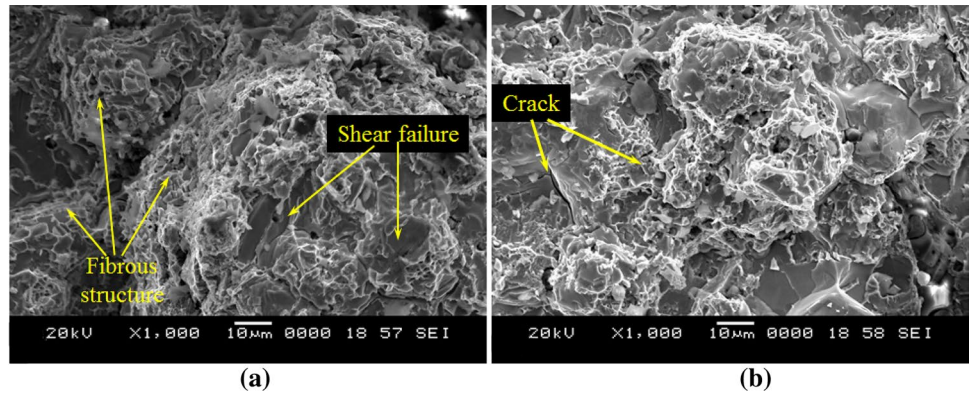


Fig. 11 SEM micrograph and EDS analysis in fusion zone of Inconel-625 specimen welded at 600 W

Table 13 Elemental composition and Laves volume fraction

Power used for processing, W	Element, wt.%								Laves phase vol. fraction, (%)
	Ni	Cr	C	Fe	Nb	Ti	Mo	Si	
600	49.38	16.59	10.8	2.86	11.64	0.98	5.68	0.87	11.5±1.4
900	46.71	15.73	11.6	3.49	13.87	1.09	6.23	1.07	15.6±1.2

Fig. 12 SEM micrographs of fractured specimens processed at (a) 600 W (b) 900 W



Conclusions

Inconel-625 plates of 6 mm thickness were joined successfully through MHH process using nickel-based powder as interface filler and investigation of process parameters influencing the UTS and FS of the microwave-induced joints is made. The optimization of multi-performance characteristics of welding through MHH technique is carried out through GRA. Based on the experimentation, following conclusions have been drawn.

1. Application of Taguchi method reveals that use of finer interface filler powder size with APS 50 micron improves strength of the joint.
2. The optimum combination of process parameters obtained through GRA was observed as separator with combination of graphite and flux followed by coal susceptor and 50 micron (APS) filler powder.
3. Based on ANOVA results of grey relational grade it is further observed that interface filler powder is the most significant parameter followed by separator and susceptor.
4. Confirmation experiment results are found to be in agreement with that of predicted results.
5. As revealed by SEM and EDS analysis, specimens processed with 600 W power exhibit better microstructural characteristics and superior strength compared to those processed with 900 W. This is attributed to the lower amount of Laves phase volume fraction observed with welded joints processed with 600 W power which further validates the results obtained through optimization process.

References

1. S.K. Rai, A. Kumar, V. Shankar, T. Jayakumar, K.B.S. Rao, B. Raj, Characterization of microstructures in Inconel 625 using X-ray diffraction peak broadening and lattice parameter measurements. *Scr. Mater.* **51**(1), 59–63 (2004)
2. H.Z. Rajani, S.A. Mousavi, The effect of explosive welding parameters on metallurgical and mechanical interfacial features of Inconel 625/plain carbon steel bimetal plate. *Mater. Sci. Eng., A* **556**, 454–464 (2012)
3. M.B. Henderson, D. Arrell, M. Heobel, R. Larsson, G. Marchant, Nickel-based superalloy welding practices for industrial gas turbine applications. *Sci. Technol. Weld. Join.* **9**(1), 13–21 (2004)
4. D.E. Clark, W.H. Sutton, Microwave processing of materials. *Annu. Rev. Mater. Sci.* **26**(1), 299–331 (1996)
5. M. Gupta, E.W. Leong, *Microwaves and metals* (Wiley, Hoboken, 2008), p. 67
6. A.K. Sharma, M.S. Srinath, P. Kumar, Indian patent 1994/Del/2009 (2009)
7. M.S. Srinath, A.K. Sharma, P. Kumar, A new approach to joining of bulk copper using microwave energy. *Mater. Des.* **32**(5), 2685–2694 (2011)
8. M.S. Srinath, A.K. Sharma, P. Kumar, Investigation on microstructural and mechanical properties of microwave processed dissimilar joints. *J. Manuf. Process.* **13**, 141–146 (2011)
9. A. Bansal, A.K. Sharma, S. Das, P. Kumar, On microstructure and strength properties of microwave welded Inconel 718/stainless steel (SS-316L). *Proc. Inst. Mech. Eng., L J. Mater. Des. Appl.* **230**(5), 939–948 (2016)
10. A. Bansal, A.K. Sharma, P. Kumar, S. Das, Structure-property correlations in microwave joining of Inconel 718. *J. Miner. Met. Mater. Soc. (TMS)* **67**(9), 2087–2098 (2015)
11. R.I. Badiger, S. Narendranath, M.S. Srinath, Microstructure and mechanical properties of Inconel-625 welded joint developed through microwave hybrid heating. *Proc. Inst. Mech. Eng., B J. Eng. Manuf.* **232**(14), 2462–2477 (2017)
12. A.K. Lakshminarayanan, V. Balasubramanian, Process parameters optimization for friction stir welding of RDE-40 aluminium alloy using Taguchi technique. *Trans. Nonferrous Met. Soc. China* **18**, 548–554 (2008)
13. H.L. Lin, Optimization of Inconel 718 alloy welds in an activated GTA welding via Taguchi method, gray relational analysis, and a neural network. *Int. J. Adv. Manuf. Technol.* **67**(1–4), 939–950 (2013)
14. C.N. Patel, S.A. Chaudhary, Parametric optimization of weld strength of metal inert gas welding and tungsten inert gas welding by using analysis of variance and grey relational analysis. *Int. J. Res. Mod. Eng. Emerg. Technol.* **1**(3), 48–56 (2013)
15. S. Ilo, C. Just, F. Xhiku, Optimisation of multiple quality characteristics of hardfacing using grey-based Taguchi method. *Mater. Des.* **33**, 459–468 (2012)
16. B.N. Ramesh, B. Suresha, Optimization of tribological parameters in abrasive wear mode of carbon-epoxy hybrid composites. *Mater. Des.* **31**(59), 38–49 (2014)
17. K.S. Prasad, S.R. Chalamalasetti, N.R. Damera, Application of grey relational analysis for optimizing weld bead geometry parameters of pulsed current micro plasma arc welded Inconel 625 sheets. *Int. J. Adv. Manuf. Technol.* **78**, 625–632 (2015)
18. G. Padmanaban, V. Balasubramanian, Optimization of pulsed current gas tungsten arc welding process parameters to attain maximum tensile strength in AZ31B magnesium alloy. *Trans. Nonferrous Met. Soc. China* **21**(3), 467–476 (2011)
19. K.S. Prasad, C.S. Rao, D.N. Rao, Optimization of fusion zone grain size, hardness, and ultimate tensile strength of pulsed current micro plasma arc welded Inconel 625 sheets using genetic algorithm. *Int. J. Adv. Manuf. Technol.* **85**, 2287–2295 (2016)
20. A.K. Srirangan, S. Paulraj, Multi-response optimization of process parameters for TIG welding of Incoloy 800HT by Taguchi grey relational analysis. *Eng. Sci. Technol. Int. J.* **19**(2), 811–817 (2016)
21. B. Shanmugarajan, R. Shrivastava, P. Sathiy, G. Buvanashkaran, Optimisation of laser welding parameters for welding of P92 material using Taguchi based grey relational analysis. *Def. Technol.* **12**(4), 343–350 (2016)
22. S.P. Dwivedi, S. Sharma, Effect of process parameters on tensile strength of 1018 mild steel joints fabricated by microwave welding. *Metallog. Microstruct. Anal.* **3**(1), 58–69 (2014)
23. A.M. Hebbale, M.S. Srinath, Taguchi analysis on erosive wear behavior of cobalt based microwave cladding on stainless steel AISI-420. *Measurement* **99**, 98–107 (2017)
24. A. Mondal, D. Agrawal, A. Upadhyaya, Microwave heating of pure copper powder with varying particle size and porosity. *J. Microw. Power Electromagn. Energy* **43**(1), 5–10 (2008)
25. N. Yoshikawa, E. Ishizuka, S. Taniguchi, Heating of metal particles in a single-mode microwave applicator. *Mater. Trans.* **47**(3), 898–902 (2006)
26. C.A. Crane, M.L. Pantoya, B.L. Weeks, M. Saed, The effects of particle size on microwave heating of metal and metal oxide powders. *Powder Technol.* **256**, 113–117 (2014)

27. L. Bagha, S. Sehgal, A. Thakur, H. Kumar, Effects of powder size of interface material on selective hybrid carbon microwave joining of SS304-SS304. *J. Manuf. Process.* **25**, 290–295 (2017)
28. A. Dey, S. Debnath, K.M. Pandey, Optimization of electrical discharge machining process parameters for Al6061/cenosphere composite using grey-based hybrid approach. *Trans. Nonferrous Met. Soc. China* **27**(5), 998–1010 (2017)
29. J.N. DuPont, M.R. Notis, A.R. Marder, C.V. Robino, J.R. Michael, Solidification of Nb-bearing superalloys: part I. Reaction sequences. *Metall. Mater. Trans. A* **29**(11), 2785–2796 (1998)
30. R.D. Peelamedu, R. Roy, D.K. Agrawal, Microwave induced reaction sintering of Ni aluminates. *Mater. Lett.* **55**, 234–240 (2002)
31. G.D. Janaki Ram, A. Venugopal Reddy, K. Prasad Rao, G. Madhusudhan Reddy, Control of Laves phase in Inconel 718 GTA welds with current pulsing. *Sci. Technol. Weld. Join.* **9**(5), 390–398 (2004)